Annually Resolved Monsoon Onset and Withdrawal Dates Across the Himalayas Derived From Local Precipitation Statistics

C. Brunello, C. Andermann, O. Marc, K. Schneider, F. Comiti, S. Achleitner, N. Hovius

Geophysical Research Letters

RESEARCH LETTER
10.1029/2020GL088420

Annually Resolved Monsoon Onset and Withdrawal Dates Across the Himalayas Derived From Local Precipitation Statistics

C. F. Brunello[1,2], C. Andermann[1], O. Marc[3,4], K. A. Schneider[1,5], F. Comiti[2], S. Achleitner[5], and N. Hovius[1,6]

[1]Helmholtz Centre Potsdam, German Research Centre for Geosciences, Potsdam, Germany, [2]Faculty of Science and Technology, Free University of Bozen-Bolzano, Bozen-Bolzano, Italy, [3]Géosciences Environnement Toulouse (GET), UMR 5563, CNRS/IRD/UPS/CNES, Observatoire Midi-Pyrénées, Toulouse, France, [4]Geological Institute, ETH Swiss Federal Institute of Technology Zurich, Zurich, Switzerland, [5]Department of Hydraulic Engineering, Institute for Infrastructure, University of Innsbruck, Innsbruck, Austria, [6]Institute of Earth and Environmental Science, University of Potsdam, Potsdam-Golm, Germany

Key Points:
- We propose a new statistical definition of monsoon onset and withdrawal applicable a posteriori to daily precipitation time series
- Monsoon bounds show longitudinal delays and strong year-to-year variations, crossing commonly used seasonal calendric boundaries
- The long-term increase of annual precipitation in Nepal seems to be driven primarily by higher premonsoon rainfall

Supporting Information:
- Supporting Information S1
- Movie S1

Correspondence to:
C. F. Brunello,
camilla.brunello@gfz-potsdam.de

Citation:
Brunello, C. F., Andermann, C., Marc, O., Schneider, K. A., Comiti, F., Achleitner, S., & Hovius, N. (2020). Annually resolved monsoon onset and withdrawal dates across the Himalayas derived from local precipitation statistics. *Geophysical Research Letters*, *47*, e2020GL088420. https://doi.org/10.1029/2020GL088420

Received 16 APR 2020
Accepted 17 NOV 2020
Accepted article online 23 NOV 2020

Abstract A local and flexible definition of the monsoon season based on hydrological evidence is important for the understanding and management of Himalayan water resources. Here, we present an objective statistical method to retrieve seasonal hydrometeorological transitions. Applied to daily rainfall data (1951–2015), this method shows an average longitudinal delay of ~15 days, with later monsoon onset and earlier withdrawal in the western Himalaya, consistent with the continental progression of wet air masses. This delay leads to seasons of different length along the Himalaya and biased precipitation amounts when using uniform calendric monsoon boundaries. In the Central Himalaya annual precipitation has increased, due primarily to an increase of premonsoon precipitation. These findings highlight issues associated with a static definition of monsoon boundaries and call for a deeper understanding of nonmonsoonal precipitation over the Himalayan water tower.

Plain Language Summary Precipitation in the Himalayas determines water availability for the Indian foreland with large socioeconomic implications. Despite its importance, spatial and temporal patterns of precipitation are poorly understood. Here, we estimate the long-term average and trends of seasonal precipitation at the scale of individual catchments draining the Himalayas. We apply a statistical method to detect the timing of hydrometeorological seasons from local precipitation measurements, focusing on monsoon onset and withdrawal. We identify longitudinal and latitudinal delays, resulting in seasons of different length along and across the Himalayas. These spatial patterns and the annual variability of the monsoon boundaries mean that oft-used, fixed calendric dates, for example, 1 June to 30 September, may be inadequate for retrieving monsoon rainfall totals. Moreover, we find that, despite its prominent contribution to annual rainfall totals, the Indian summer monsoon cannot explain the increase of the annual precipitation over the Central Himalayas. Instead, this appears to be mostly driven by changes in premonsoon and winter rainfall. So far, little attention has been paid to premonsoon precipitation, but governed by evaporative processes and surface water availability, it may be enhanced by irrigation and changed land use in the Gangetic foreland.

1. Introduction

The Indian summer monsoon (ISM) is the dominant climatological phenomenon in large parts of Asia, with intense continental rainout from wet oceanic air masses. Precipitation rates are especially high across the orographic gradient of the Himalayas (Bookhagen & Burbank, 2006, 2010). There, monsoon precipitation modulates the intensity of hazardous geophysical processes such as landsliding, debris flows, and flooding —with associated erosional and depositional dynamics (e.g., Gabet et al., 2008; Marc et al., 2019; Struck et al., 2015)—and governs the availability of water sustaining food, energy, and biodiversity in the densely populated piedmont regions and adjacent plains (e.g., Immerzeel et al., 2020). Efficient management of these hazards and resources requires location-specific knowledge of the onset and end of ISM precipitation, in addition to its intensity and amount.

Water stable isotope signatures suggest that the Himalayan hydroclimate has three distinct rainfall seasons: premonsoon, monsoon, and winter (Brunello et al., 2019; Tian et al., 2020; Yao et al., 2013), reflecting different moisture sources and/or transport and condensation mechanisms (Galewsky et al., 2016). However, without isotopic data, finding the transition between these seasons is challenging. Especially, the timing of monsoon onset in the Himalayas and its variability remain poorly understood. One issue is that a nonnegligible amount of precipitation falls in the preceding period, during intermittent convective storms fed by evaporation of surface water in the Indo-Gangetic plains (Tuinenburg et al., 2012). The transition to a synoptic system with an offshore moisture source, the monsoon onset, and the transition from monsoon to the mostly dry postmonsoon season, monsoon withdrawal, are not synchronous across the region, nor do they occur at the same time every year.

Synoptic atmospheric precursors have been used to develop diagnostic indices for the regional monsoon onset and withdrawal dates (e.g., Ananthakrishnan & Soman, 1988; Boos & Emanuel, 2009; Fasullo & Webster, 2003; Joseph et al., 2006; Ordoñez et al., 2016; Taniguchi & Koike, 2006; Xavier et al., 2007). These indices report a considerable temporal variability of the regional monsoon onset, but none of them accounts for the progressive migration of monsoon rainfall. Meanwhile, spatial variability in the monsoon timing has been constrained by averaging rainfall patterns over decades to obtain climatological mean onset and withdrawal dates for specific regions (e.g., Lau & Yang, 1997; Misra et al., 2018; Murakami & Matsumoto, 1994). Only few studies have investigated the local, interannual variability of onset and withdrawal in Asia (Bombardi et al., 2020). They have considered deviations from the climatological mean (e.g., Noska & Misra, 2016) or implemented user-defined thresholds (e.g., Moron et al., 2017; Wang & LinHo, 2002). However, climatological constraints are poor in the Himalayas, and complex terrain impedes the use of given thresholds. Using an alternative approach, Cook and Buckley (2009) fitted a two-phase regression model on annual cumulative rainfall. Unfortunately, this data-driven method is less efficient where the annual cycle is not well defined or includes multiple wet seasons. Hence, an objective, local, and precipitation-based definition of the monsoon season in the Himalayas is lacking. To date, hydrological and geomorphic processes are mostly interpreted through the lens of the ISM, but in absence of objective monsoon demarcation, the large majority of studies relies on simplistic fixed calendric boundaries (e.g., 1 June to 30 September), applied uniformly throughout the vast ISM domain. This hampers our ability to capture the complexity of the Himalayan hydroclimate, its past variability, current state, and future development.

Here, we propose a straight-forward approach to overcome semiarbitrary, consensus-based calendric boundaries, which are commonly used in studies focusing on the consequences of rainfall. First, we present a hydrometeorologically based definition of the monsoon season over the Himalayas and an explicit local criterion for its demarcation. Then, we apply this method to estimate seasonal precipitation amounts, map their offset from calendric estimates, and examine seasonal precipitation trends.

2. Methods

2.1. Statistical Definition of Monsoon Boundaries

The monsoon season is characterized by intense and sustained rainfall during several months. In contrast, the premonsoon and postmonsoon seasons are drier with more erratic, often convective precipitation. To detect the transition between these seasons, we used two statistical tests for differences in precipitation amount and intensity distribution in time series measurements: the Kolmogorov-Smirnov (KS) and Wilcoxon-Mann-Whitney (WMW) tests. The former characterizes the difference between the empirical distribution functions of two samples, and the latter determines whether two independent samples have the same median value. Importantly, these two tests are nonparametric; they do not require the sample to follow any specific probability distribution. As they address different characteristics of time series, we combined the two tests into an integrated index reflecting the (dis)similarity of time series rainfall measurements (hereafter WiKS).

The KS and WMW tests were applied over moving windows with half width of 20, 30, and 40 days. The p values for the different window lengths, giving the likelihood that the two halves of the window have the same empirical cumulative distribution (KS) and median (WMW), were averaged to minimize the dependence on a specific time scale. While the KS test is sensitive to both monsoon onset and withdrawal,

the WMW test must be run twice, testing for increase (onset) and decrease (withdrawal) in median precipitation. Concatenating statistical tests, a continuous time series of p values (p_{WMW} and p_{KS}) was obtained, reflecting the significance of the difference between the precipitation occurring before and after a given date. This analysis was carried out for all days between 1 May and 31 October (Figure 1a). For more than 50% of all cases, the two tests yielded identical results (section S1 in the supporting information). In the other cases we defined WiKS as their normalized sum:

$$WiKS = \frac{log_{10}(p_{KS})}{min(log_{10}(p_{KS}))} + \frac{log_{10}(p_{WMW})}{min(log_{10}(p_{WMW}))}. \quad (1)$$

The monsoon onset and withdrawal dates are defined as the dates when WiKS is highest, with p_{WMW} tested for an increase or decrease in median, respectively. Due to insufficient data, the start and end of the winter season could not be defined in the same dynamical manner. Therefore, we defined premonsoon (1 March to onset), monsoon (onset to withdrawal), postmonsoon (withdrawal to 30 November), and winter (1 December to 28 February).

2.2. Data Set and Spatiotemporal Analysis

We used the APHRODITE-MA (Asian Precipitation Highly Resolved Observational Data Integration Towards Evaluation of Water Resources—Monsoon Region; Yatagai et al., 2012) product. With daily data from 1951–2015, APHRODITE-MA is the longest running precipitation data set available for the Himalayas. It has been shown to capture correctly the seasonal rainfall patterns in the Himalayas (Andermann et al., 2011), and the length of the record allows for systematic analysis of spatiotemporal patterns in monsoon onset and withdrawal. The version used here (V1801_R1 MA) has a spatial resolution of 0.25°.

To assess the sensitivity of WiKS to the chosen precipitation product, analyses were also conducted on the GPM IMERGHHv6B data set This is the most recent remotely sensed precipitation product, delivering satellite-based rainfall estimates with an ~10 km spatial and 30 min temporal resolution compiled to daily data (Skofronick-Jackson et al., 2017).

To analyze changes in precipitation within their hydrological context, we divided the Himalayan domain, excluding the Indus and Yarlung-Tsangpo-Brahmaputra rivers, into 24 Trans Himalayan Catchments (THCs) (Figure 1b; Table S1). Acknowledging the first-order effect of the orographic barrier, the THCs were partitioned into two subcatchments: a wet, monsoon exposed part south of the High-Himalayan peaks and a leeward, dryer part to the North. For this purpose, we used the 500 mm/year isohyet, extracted from the TRMM 2B31 climatology of Bookhagen and Burbank (2010), which traces the High-Himalayan ridgeline. This definition yields some very small northern subcatchments, where rainfall estimates may be more uncertain due to a paucity of precipitation gauges. However, precipitation errors for some single catchments should not bias the overall conclusions at the regional scale, which is the focus of our study.

Seasonal precipitation amounts were obtained within dynamic WiKS monsoon boundaries, for individual years and catchments. The presence and magnitude of long-term linear trends in annual and seasonal precipitation totals were explored using the nonparametric Mann-Kendall test and Sen's slope test (Sen, 1968) respectively. To compare catchments with different rainfall amounts, we report the total change over 1951–2015 normalized by the long-term mean. We limited this trend analyses to 10 catchments in Nepal, where the APHRODITE gauge network is most dense, stable, and long-lived (section S2).

3. Spatial Variability of Climatological Monsoon Timing

3.1. Spatial Variability of Monsoon Boundaries

Spatial patterns in the average monsoon onset and withdrawal dates reflect the distance of the monsoon front to its principal moisture source, the Bay of Bengal.

The long-term mean onset date of monsoon in the 24 THCs exhibits both longitudinal and latitudinal variations. The earliest onset (30 May, Day 150) occurs in the southern part of the easternmost basin and the latest (24 June, Day 175) in the northern part of the westernmost basin (Figure 2a). Both the southern and the northern subcatchments exhibit a delay of 15 days along the length of the range. An average lag time of

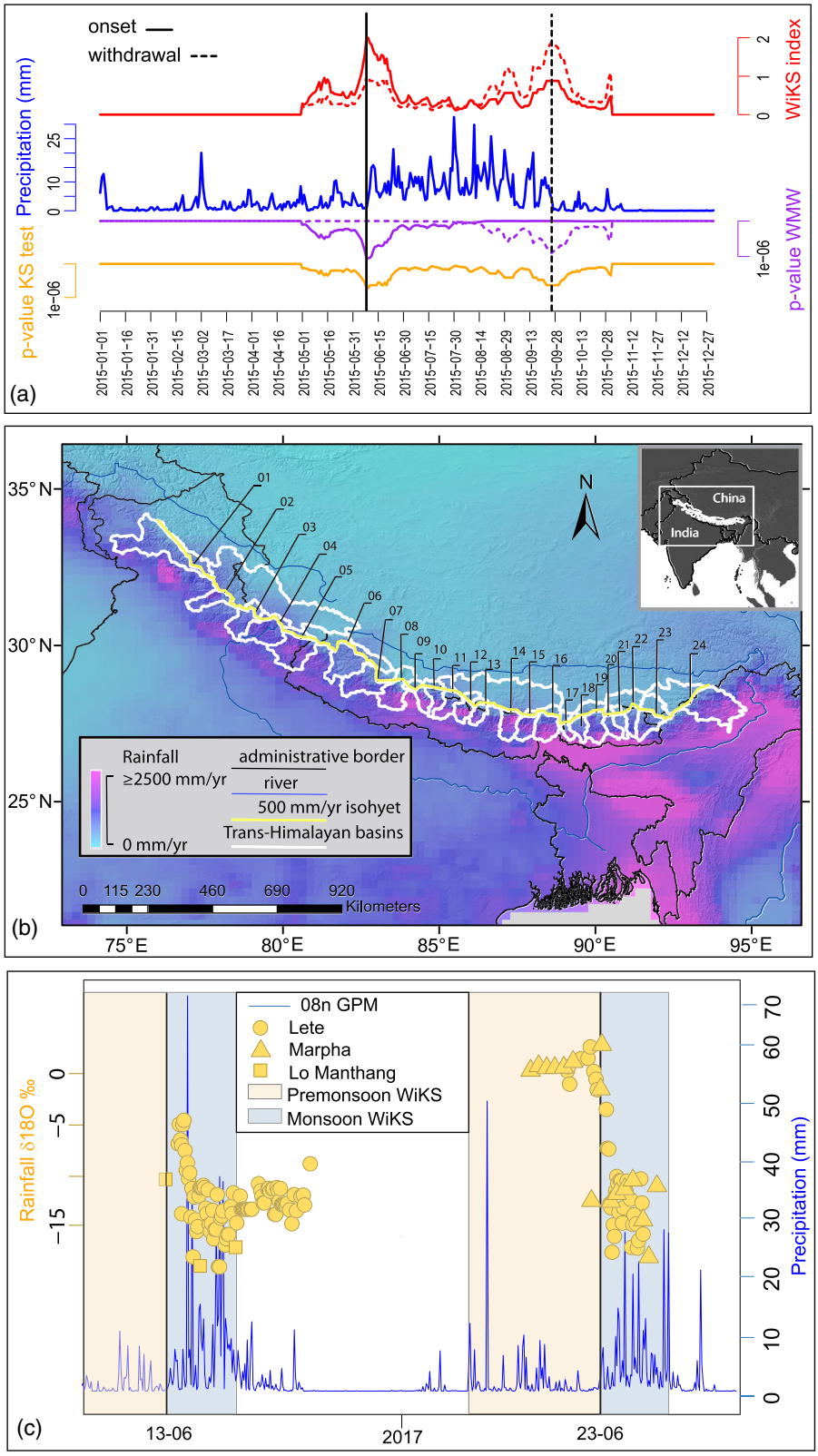

Figure 1. (a) One-year time series of daily precipitation, *p* values of Kolmogorov-Smirnoff and Wilcoxon-Mann-Whitney tests, and the normalized sum of these two tests (WiKS). Black lines show monsoon boundaries, picked at the WiKS maxima. (b) Map of mean annual precipitation with outlines of 24 Trans-Himalayan Catchments (see names in Table S1). (c) Time series of daily GPM precipitation and rainfall $\delta^{18}O$ in the upper Kali Gandaki valley (08n).

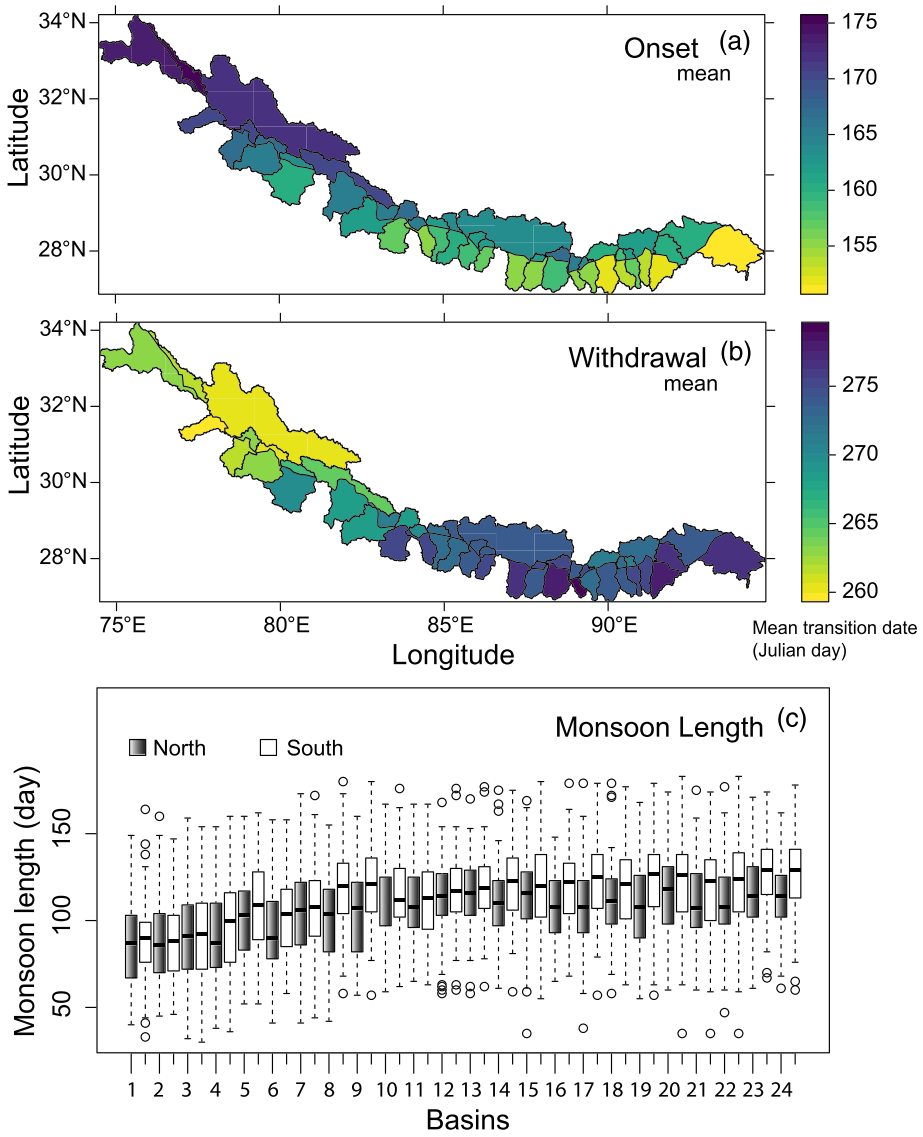

Figure 2. Long-term (1951–2015) mean monsoon onset (a) and withdrawal (b) dates in Julian days and distribution of monsoon length over the 24 THCs (c).

~6 days (min = 1, max = 11) is observed between southern and northern subcatchments. It is larger in the east (~10 days) and smaller in the west (~2 days), with intermediate values in the center. Similar but spatially reversed results were found for the mean monsoon withdrawal dates. Withdrawal occurs first in the northwestern catchments (16 September, Day 259) and last in the southeast (7 October, Day 280) (Figure 2b). Monsoon withdrawal starts ~2 days (min = −2, max = 6.6) earlier in the northern subcatchments, without a clear longitudinal trend in the north-south delay.

The lack of independent data sets describing the arrival and withdrawal of monsoon rainfall at local scale hampers the benchmarking of our results. However, similar delays are observed for GPM monsoon boundaries, although the details often differ and interannual correlation values are low (section S3). Moreover, the large-scale longitudinal gradients retrieved by our method are in general agreement with the reported normal dates of Southwest monsoon onset over India (IMD, 2020). Our observations match the regional progression of moisture evident in the long-term mean daily rainfall through the year (Movie S1). Additional independent validation of the WiKS monsoon definition comes from a comparison with rainfall $\delta^{18}O$ (Figure 1c), in the High Himalayas of Central Nepal for May 2016 to September 2017 (sampling details in

Brunello et al., 2019). Premonsoonal isotopic values are relatively high (~0‰), reflecting the contribution of continentally recycled moisture. They drop abruptly (approximately −15‰) when the precipitation intensifies, which, in turn, is identified by WiKS as the monsoon onset. In 2017, the coincidence of the isotopic shift and the WiKS monsoon onset on 23 June suggests that our statistically derived monsoon boundaries are indeed linked to the inflow of isotopically depleted oceanic air masses.

The regional-scale atmospheric monsoon onset is often assumed to manifest in a substantial local-scale increase of rainfall. To test this, we have assessed the correlation between our catchment-wide onset dates and several published monsoon onset indices (Ananthakrishnan & Soman, 1988, AS; Joseph et al., 2006, IMD; Fasullo & Webster, 2003; Taniguchi & Koike, 2006; Xavier et al., 2007). These correlations reach only moderate values ($r = 0.3$–0.5) and are nonuniform across the Himalayan domain (section S4). Although better matches are achieved in specific subregions, no agreement is found across the mountain belt. Indices based on synoptic atmospheric precursors better match the local precipitation patterns in the western Himalaya, while the local increase in rainfall in southernmost India (AS, IMD) has a better correlation with the southeastern THCs. Moreover, regional onset estimates may correlate with the local onset in southern subcatchments, but more rarely in northern ones. This is consistent with our estimated delays across the orographic barrier. Our results indicate that regional-scale monsoon indices do not systematically relate to rainout over the Himalayan catchments, as also found by Moron and Robertson (2014) and Bombardi et al. (2020). Therefore, we suggest that even if regional-scale monsoon onset can start local-scale monsoon rainfall, the latter results from smaller scale processes, which are poorly reproducible from one year to another.

3.2. Spatial Variability of Monsoon Length

Monsoon rain is delivered earlier in the east, closer to the predominant source in the Bay of Bengal, and later farther west. This reflects the migration of the monsoon front along the Himalayan range. During monsoon withdrawal, the inflow of the oceanic air masses weakens, first in the west and then farther east. Over its length, the mountain belt retards the monsoon migration at the onset, while the withdrawal of the monsoon is not affected by orography, with minimal north-south delays. Central Nepal, where the ridgeline comprises the highest mountains, has the strongest S-N onset delays. Onset delays are also relatively large in Bhutanese catchments (20–22) leeward of the Shillong Plateau, which blocks the northward progression of moisture (e.g., Grujic et al., 2006). Thus, on top of the well-described effect on precipitation distribution (e.g., Anders et al., 2006), Himalayan orography determines the timing of precipitation.

The observed regional monsoon dynamic results in meteorological seasons with different length along the Himalayas (Figure 2c). The average length of the monsoon season in the THCs is 110 days, with a maximum deviation of 37 days. The monsoon is shortest in the west, around 90 days, with little difference in season length across the orographic barrier. In the central Himalayas (84°–87°E) the monsoon lasts around 100–110 days, and in the east (87°–94° E) the contrast between north and south is the strongest, the monsoon season lasting around 110 days in the north and >120 days south in the south.

4. Spatiotemporal Precipitation Estimates

4.1. Seasonal Precipitation Estimates

WiKS is a data-driven method to allocate precipitation to the relevant hydrometeorological seasons. It facilitates investigation of seasonal precipitation budgets. To assess the relative bias introduced by fixed boundaries, we compute the difference between seasonal precipitation estimates for WiKS and the most common calendric boundaries (1 June to 30 September), normalized by annual rainfall. Interannual correlations are reported in section S5. Calendric partitioning is common practice in the assessment of spatiotemporal variability of monsoon amounts by end-users; here, we illustrate the magnitude and distribution of errors associated with this approach. Given the minor significance of postmonsoon and the static definition of Winter, we focus on premonsoon and monsoon precipitation estimates.

The normalized difference in monsoon precipitation is shown in Figure 3. In the northern subcatchments, differences range from −34% to +30%. Calendric seasons yield larger monsoon precipitation amounts, with negative average differences during 1951–2015 in all basins except THCs 12 and 13. This difference increases

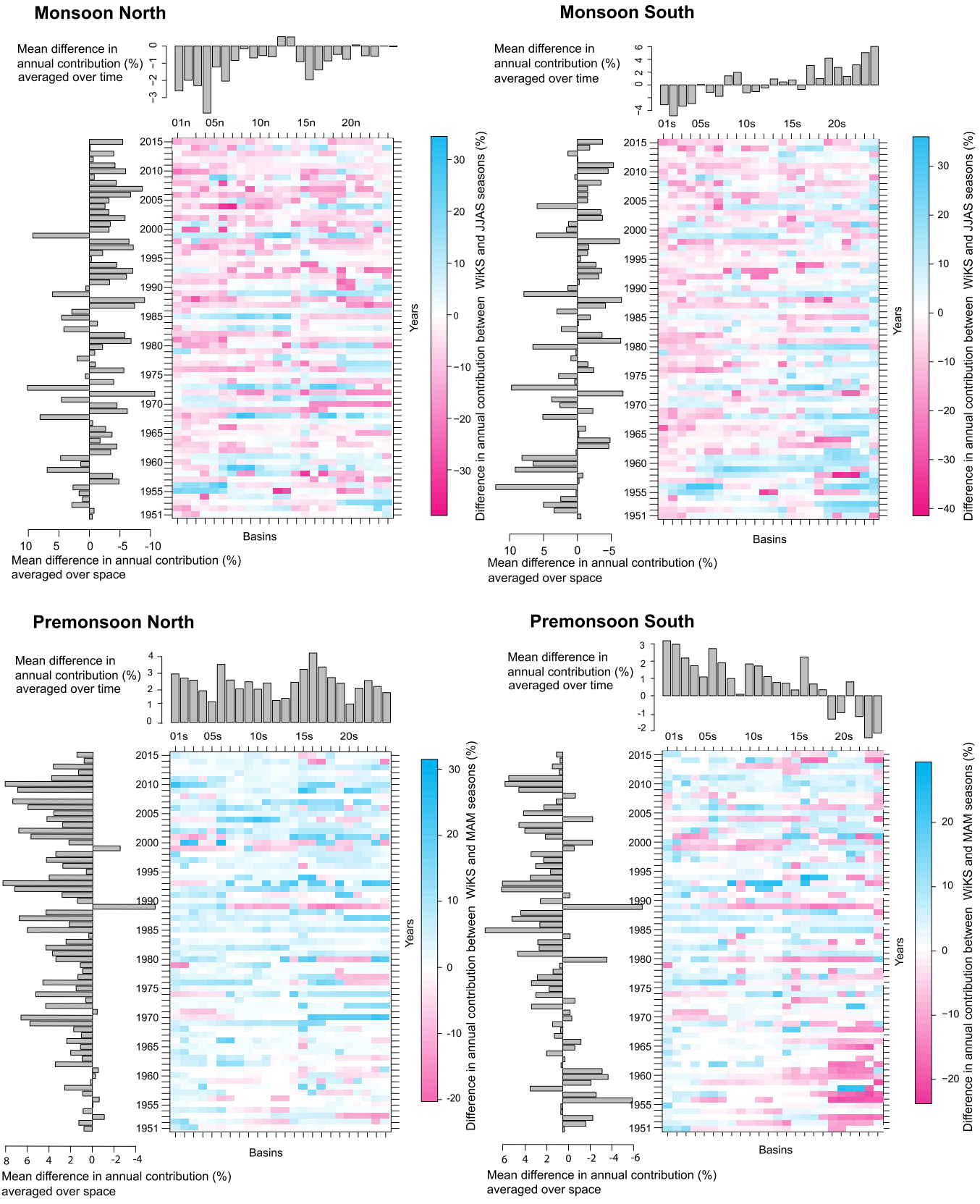

Figure 3. Differences in monsoon and premonsoon precipitation totals for WiKS and calendric seasons, shown as heat maps with THCs on *x* axes and years on *y* axis. Values are reported as percentage of the total annual precipitation.

westward. Some years had spatially consistent positive differences (e.g., 1999 and 1973); in others differences were uniformly negative (e.g., 1988 and 1972).

In the southern subcatchments, normalized differences range from −37% to +32%. In the eastern catchments, WiKS monsoons have, on average, more rain than calendric monsoons. In the central Himalayas, values are similar, and in the west, the differences are mostly negative, because the WiKS monsoon is shorter than the calendric one. In terms of temporal evolution, in the first decades of record, calendric seasons consistently yield smaller rainfall totals, by up to 10% compared to WiKS; cases with WiKS rain estimates lower than the calendric estimates are sparse with small deviations, less than~5%.

Normalized premonsoon precipitation differences are computed using calendric (1 March to 31 May) and mixed calendric-WiKS (1 March to onset) seasonal bounds. In northern subcatchments, WikS-based estimates are, on average, higher (2.6%, min = −17%, max = 28%). No significant spatial patterns are observed, and all basins show positive time-averaged differences ranging from 1.2% to 4.7%. However, a progressive increase of WiKS values compared to calendric estimates is observed since 1951, with differences frequently >7% in the last two decades.

For the southern subcatchments, the spatially averaged differences between mixed calendric-WiKs and purely calendric estimates are minor, less than ±6%. However, individual differences range from −20.5% to 26%, with negative differences in the early part of the record (~1960–1995) in the eastern catchments, grading progressively to proportionally higher WiKS rainfall westward.

Only in the Central Himalayas the long-term mean calendric- and WiKS-based estimates of monsoon rain totals are similar (±1%). Elsewhere, calendric season bounds do not permit an adequate attribution of precipitation to the correct season. Systematic differences between calendric- and WiKS-based monsoon precipitation estimates reflect the important longitudinal gradient in the season length. Notably, in specific catchments and years, the difference between precipitation estimates exceeds 40% of the annual total. Thus, the use of calendric monsoon precipitation estimates can be a major source of error in studies of precipitation-driven processes at seasonal time scales. The lack of a systematic change in time of the offset between calendric- and WiKS-based monsoon estimates suggests that from 1951 monsoon length variations oscillated around a stable mean. Meanwhile, the difference of premonsoon precipitation estimated with mixed and calendric bounds has risen from −3% to 4%, indicating strengthening and/or lengthening of the WiKS-based premonsoon.

4.2. Seasonal Precipitation Trends

We have demonstrated a significant variability of monsoon onset and withdrawal dates (Figure 2) and calculated long-term average seasonal rainfall totals (Figure 3). Next, we perform trend analysis of seasonal precipitation amounts in 10 Nepalese catchments (Figure 4a), where the dense and long-lived gauging network maximizes Aphrodite's reliability.

Long-term trends were obtained by applying Mann-Kendall and Sen's slope tests on annual and seasonal precipitation totals (1951–2015) (Figure 4b). Annual rainfall in Nepal has increased by 8–30 mm, on both sides of the orographic barrier, except Catchments 7 and 8, where precipitation decreased north of the barrier (8–11 mm). This trend in annual rainfall is primarily due to spatially consistent changes during the premonsoon. Premonsoon precipitation totals have increased by 54–124 mm relative to 1951, complemented by an ~11–70 mm increase in winter precipitation, especially in northern subcatchments. Meanwhile, monsoon precipitation in northern Subcatchments 6–10 decreased by 110–153 mm.

Long-term trends in mean premonsoon rainfall intensity (in mm/day) and premonsoon seasonal length suggest that intensification of daily precipitation dominates (~80%) the augmented rainfall depth during the premonsoon period, while season lengthening plays subsidiary role (Figure 4c). These proportions were obtained by computing how much of the long-term total rainfall increase would be caused by each of these terms, as derived from their Sen's slope, assuming the other constant.

We note that the significance of the long-term premonsoon trend is due to a ramp-like increase of reported precipitation during the first 30 years of the record. The first decade, 1951–1961, has a low observation density, and trends computed only for the better monitored interval 1961–2015 are not statistically significant (section S2; Figure S3). However, Kamiguchi et al. (2010) and Hofstra et al. (2010) demonstrated that

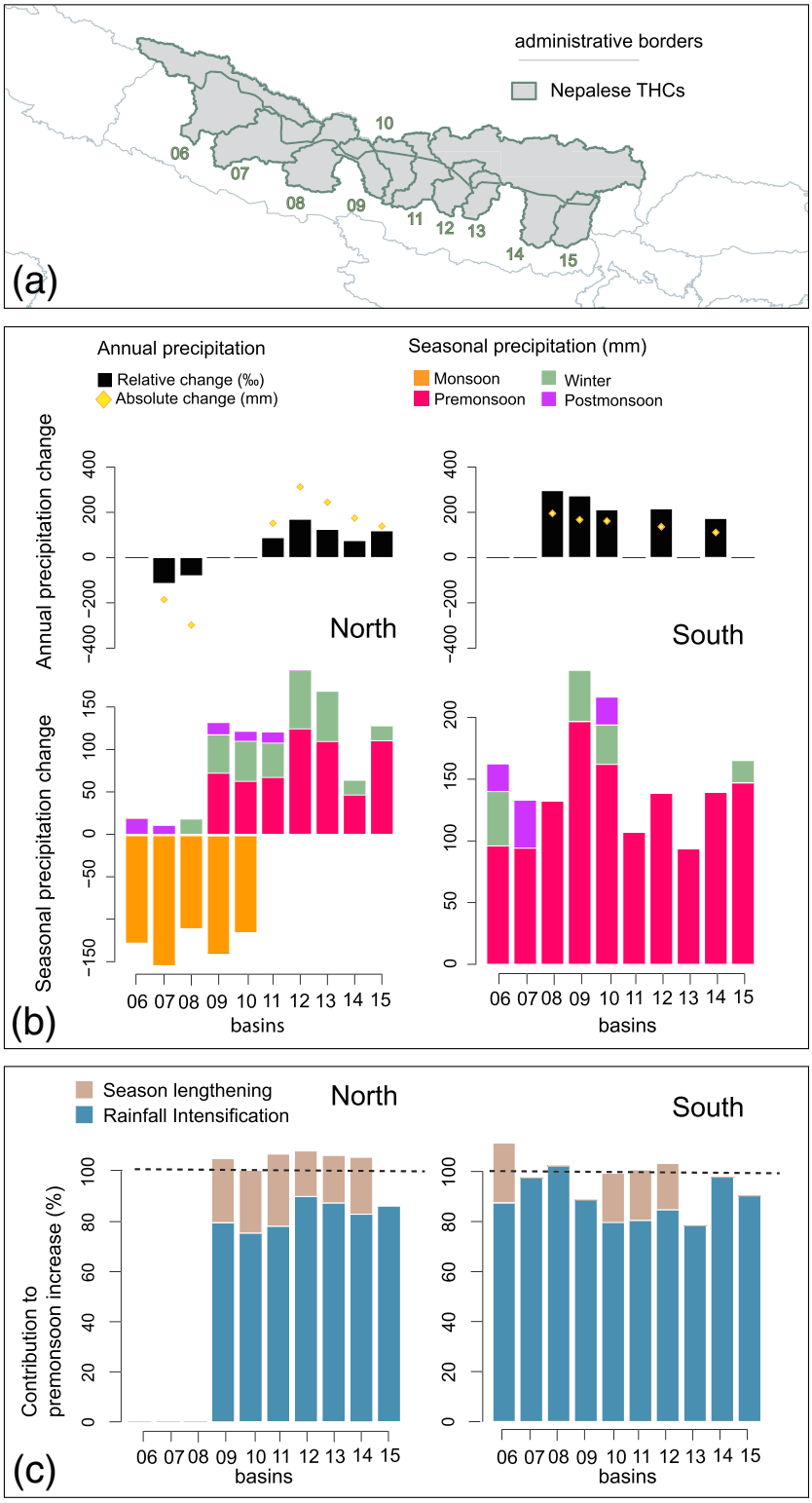

Figure 4. Seasonal precipitation changes in the Nepalese THCs (a) expressed as linear monotonic change of annual and seasonal precipitation (b) and proportion of the premonsoon increase due to season lengthening and mean rainfall intensification (c) over 1951–2015. In b and c, only Sen's slope values with Mann Kendall test $p < 0.05$ are reported.

temporal changes in the gauge network coverage have no effect on the seasonal precipitation amounts but only on frequency-intensity distribution. Still, caution is needed when interpreting precipitation data from a variable number of stations, and any premonsoon precipitation changes remain to be validated (section S2).

Our results highlight an important and previously unreported aspect of the Himalayan hydroclimate: the dominant role of rainfall during nonmonsoonal seasons in driving the evolution of the annual precipitation amount, in spite of their minor absolute contribution (from west to east, 25–15% for premonsoon and 20% to 5% for winter). Most studies of Himalayan precipitation focused on the monsoon season, which dominates the regional water budget (e.g., Bookhagen & Burbank, 2010). However, for water availability and management, the premonsoon period may have considerable importance, especially because it coincides with the start of the vegetative season. Previous work relates premonsoon rain to surface water availability and evaporation in the Indo-Gangetic plain (Pradhan et al., 2019; Tuinenburg et al., 2012), consistent with the relative isotopic enrichment of premonsoon rainfall (Figure 1c). This has increased substantially in recent decades due to extensive irrigation (Cook et al., 2015; Rodell et al., 2009; Tuinenburg et al., 2014). Confirmation of their causal relationship would demonstrate human manipulation of the Himalayan water cycle. More work is needed to identify the underlying mechanisms of premonsoon rainfall and the coupling of these mechanisms with the ISM system.

5. Conclusions

To resolve the timing of monsoon on an annual scale and to assign precipitation to the correct season, we have designed an objective season delineation method (WiKS), combining two nonparametric statistical change point tests. Tailored for the Himalayas, where climatological constraints are scarce and hydroclimatic contributions complex, WiKS can be applied to any dataset with daily resolution over monsoon-dominated regions. With this method, we determined the spatiotemporal distribution of the onset and withdrawal of monsoon precipitation over the period 1951–2015 across the Himalayas. Coincidence with a drop-in rainfall $\delta^{18}O$ values in the Nepalese Himalaya suggests that WiKS monsoon onset dates are mechanistically meaningful. Ultimately, depending on the application, combining different diagnostics may provide additional insights.

WiKS monsoon boundary dates corroborate the longitudinal delay of the long-term mean monsoon onset along the Himalayan range, which results in substantially shorter monsoon duration in the west and behind the orographic barrier. Further, they enable for the first time to identify exceptional years or spatial anomalies in monsoon timing, the analysis of which may yield insights into underlying controls. Overcoming the limitations of calendric monsoon definition, WiKS can help sharpen the quantification of rainfall-driven processes in monsoon dominated regions, setting a benchmark for modeling and forecasting of annual and seasonal Himalayan monsoon rainfall.

WiKS allows an objective attribution of measured precipitation to the different seasons and therefore more robust estimates of their long-term average trends. We find a pervasive long-term increase in annual precipitation totals in the Nepal Himalayas, which cannot be attributed to the ISM. Instead, it was mainly driven by rainfall intensification during premonsoon, complemented by winter precipitation. Despite the moderate contribution to annual precipitation totals (20–45%), precipitation in nonmonsoonal seasons appears to have steered the hydroclimatic evolution of the region since the 1950s. These findings encourage a shift of attention to smaller-scale moisture sources and drivers for understanding the changes in precipitation availability over the Himalayan water tower.

Conflict of Interest

The authors do not have conflicts of interest to declare.

Data Availability Statement

The APHRODITE data set (APHRO_MA_V1801_R1) is available at http://aphrodite.st.hirosaki-u.ac.jp/products.html (last access 28.09.20). The GPM IMERGHHv6B data are available at https://pmm.nasa.gov/data-access/downloads/gpm (last access: 28.09.20). The Shuttle Radar Topography Mission-30-m digital elevation

model (NASA JPL, 2013) was retrieved from the online Global Data Explorer (https://gdex.cr.usgs.gov/gdex/, last access: 30.03.20).

Acknowledgments
We thank Vincent Moron for providing the regional monsoon indices.

References

Ananthakrishnan, R., & Soman, M. (1988). The onset of the southwest monsoon over Kerala: 1901–1980. *Journal of Climatology*, *8*(3), 283–296. https://doi.org/10.1002/joc.3370080305

Andermann, C., Bonnet, S., & Gloaguen, R. (2011). Evaluation of precipitation data sets along the Himalayan front. *Geochemistry, Geophysics, Geosystems*, *12*, Q07023. https://doi.org/10.1029/2011GC003513

Anders, A. M., Roe, G. H., Hallet, B., Montgomery, D. R., Finnegan, N. J., & Putkonen, J. (2006). Spatial patterns of precipitation and topography in the Himalaya. *Special Papers-Geological Society of America*, *398*, 39.

Bombardi, R. J., Moron, V., & Goodnight, J. S. (2020). Detection, variability, and predictability of monsoon onset and withdrawal dates: A review. *International Journal of Climatology*, *40*(2), 641–667. https://doi.org/10.1002/joc.6264

Bookhagen, B., & Burbank, D. (2010). Toward a complete Himalayan hydrological budget: Spatiotemporal distribution of snowmelt and rainfall and their impact on river discharge. *Journal of Geophysical Research*, *115*, F03019. https://doi.org/10.1029/2009JF001426

Bookhagen, B., & Burbank, D. W. (2006). Topography, relief, and TRMM-derived rainfall variations along the Himalaya. *Geophysical Research Letters*, *33*, L08405. https://doi.org/10.1029/2006GL026037

Boos, W., & Emanuel, K. (2009). Annual intensification of the Somali jet in a quasi-equilibrium framework: Observational composites. *Quarterly Journal of the Royal Meteorological Society*, *135*(639), 319–335. https://doi.org/10.1002/qj.388

Brunello, C. F., Andermann, C., Helle, G., Comiti, F., Tonon, G., Tiwari, A., & Hovius, N. (2019). Hydroclimatic seasonality recorded by tree ring δ18O signature across a Himalayan altitudinal transect. *Earth and Planetary Science Letters*, *518*, 148–159. https://doi.org/10.1016/j.epsl.2019.04.030

Cook, B., Shukla, S. P., Puma, M., & Nazarenko, L. (2015). Irrigation as an historical climate forcing. *Climate Dynamics*, *44*(5–6), 1715–1730. https://doi.org/10.1007/s00382-014-2204-7

Cook, B. I., & Buckley, B. M. (2009). Objective determination of monsoon season onset, withdrawal, and length. *Journal of Geophysical Research*, *114*, D23109. https://doi.org/10.1029/2009JD012795

Fasullo, J., & Webster, P. (2003). A hydrological definition of Indian monsoon onset and withdrawal. *Journal of Climate*, *16*(19), 3200–3211. https://doi.org/10.1175/1520-0442(2003)016<3200a:AHDOIM>2.0.CO;2

Gabet, E. J., Burbank, D. W., Pratt-Sitaula, B., Putkonen, J., & Bookhagen, B. (2008). Modern erosion rates in the High Himalayas of Nepal. *Earth and Planetary Science Letters*, *267*(3–4), 482–494. https://doi.org/10.1016/j.epsl.2007.11.059

Galewsky, J., Steen-Larsen, H. C., Field, R. D., Worden, J., Risi, C., & Schneider, M. (2016). Stable isotopes in atmospheric water vapor and applications to the hydrologic cycle. *Reviews of Geophysics*, *54*, 809–865. https://doi.org/10.1002/2015RG000512

Grujic, D., Coutand, I., Bookhagen, B., Bonnet, S., Blythe, A., & Duncan, C. (2006). Climatic forcing of erosion, landscape, and tectonics in the Bhutan Himalayas. *Geology*, *34*(10), 801–804. https://doi.org/10.1130/G22648.1

Hofstra, N., New, M., & McSweeney, C. (2010). The influence of interpolation and station network density on the distributions and trends of climate variables in gridded daily data. *Climate Dynamics*, *35*(5), 841–858. https://doi.org/10.1007/s00382-009-0698-1

IMD (2020). Indian Metrological Department, Regional Metrological Center, Nagpur, Normal dates of onset for south west monsoon, webpage (last opened: 29.03.2020). http://imdnagpur.gov.in/pages/monsoon_main.php?adta=ONSET%26adtb=%26adtc=%26adtd=onset

Immerzeel, W. W., Lutz, A. F., Andrade, M., Bahl, A., Biemans, H., Bolch, T., et al. (2020). Importance and vulnerability of the world's water towers. *Nature*, *577*(7790), 364–369. https://doi.org/10.1038/s41586-019-1822-y

Joseph, P., Sooraj, K., & Rajan, C. (2006). The summer monsoon onset process over South Asia and an objective method for the date of monsoon onset over Kerala. *International Journal of Climatology*, *26*(13), 1871–1893. https://doi.org/10.1002/joc.1340

Kamiguchi, K., Arakawa, O., Kitoh, A., Yatagai, A., Hamada, A., & Yasutomi, N. (2010). Development of APHRO_JP, the first Japanese high-resolution daily precipitation product for more than 100 years. *Hydrological Research Letters*, *4*, 60–64. https://doi.org/10.3178/hrl.4.60

Lau, K., & Yang, S. (1997). Climatology and interannual variability of the Southeast Asian summer monsoon. *Advances in Atmospheric Sciences*, *14*(2), 141–162. https://doi.org/10.1007/s00376-997-0016-y

Marc, O., Behling, R., Andermann, C., Turowski, J., Illien, L., Roessner, S., & Hovius, N. (2019). Long-term erosion of the Nepal Himalayas by bedrock landsliding: The role of monsoons, earthquakes and giant landslides. *Earth Surface Dynamics*, *7*(1), 107–128. https://doi.org/10.5194/esurf-7-107-2019

Misra, V., Bhardwaj, A., & Mishra, A. (2018). Local onset and demise of the Indian summer monsoon. *Climate Dynamics*, *51*(5–6), 1609–1622. https://doi.org/10.1007/s00382-017-3924-2

Moron, V., & Robertson, A. (2014). Interannual variability of Indian summer monsoon rainfall onset date at local scale. *International Journal of Climatology*, *34*(4), 1050–1061. https://doi.org/10.1002/joc.3745

Moron, V., Robertson, A. W., & Pai, D. S. (2017). On the spatial coherence of sub-seasonal to seasonal Indian rainfall anomalies. *Climate Dynamics*, *49*(9–10), 3403–3423. https://doi.org/10.1007/s00382-017-3520-5

Murakami, T., & Matsumoto, J. (1994). Summer monsoon over the Asian continent and western North Pacific. *Journal of the Meteorological Society of Japan Series II*, *72*(5), 719–745.

NASA JPL (2013). NASA Shuttle Radar Topography Mission Global 1 arc second [data set], NASA EOSDIS land processes DAAC.

Noska, R., & Misra, V. (2016). Characterizing the onset and demise of the Indian summer monsoon. *Geophysical Research Letters*, *43*, 4547–4554. https://doi.org/10.1002/2016GL068409

Ordoñez, P., Gallego, D., Ribera, P., Peña-Ortiz, C., & García-Herrera, R. (2016). Tracking the Indian summer monsoon onset back to the preinstrument period. *Journal of Climate*, *29*(22), 8115–8127. https://doi.org/10.1175/JCLI-D-15-0788.1

Pradhan, R., Singh, N., & Singh, R. (2019). Onset of summer monsoon in Northeast India is preceded by enhanced transpiration. *Scientific Reports*, *9*(1), 1–11.

Rodell, M., Velicogna, I., & Famiglietti, J. (2009). Satellite-based estimates of groundwater depletion in India. *Nature*, *460*(7258), 999–1002. https://doi.org/10.1038/nature08238

Sen, P. (1968). Estimates of the regression coefficient based on Kendall's tau. *Journal of the American Statistical Association*, *63*(324), 1379–1389. https://doi.org/10.1080/01621459.1968.10480934

Skofronick-Jackson, G., Petersen, W., Berg, W., Kidd, C., Stocker, E., Kirschbaum, D., et al. (2017). The global precipitation measurement (GPM) Mission for science and society. *Bulletin of the American Meteorological Society*, *98*(8), 1679–1695. https://doi.org/10.1175/BAMS-D-15-00306.1

Struck, M., Andermann, C., Hovius, N., Korup, O., Turowski, J. M., Bista, R., et al. (2015). Monsoonal hillslope processes determine grain size-specific suspended sediment fluxes in a trans-Himalayan river. *Geophysical Research Letters*, *42*, 2302–2308. https://doi.org/10.1002/2015GL063360

Taniguchi, K., & Koike, T. (2006). Comparison of definitions of Indian summer monsoon onset: Better representation of rapid transitions of atmospheric conditions. *Geophysical Research Letters*, *33*, L02709. https://doi.org/10.1029/2005GL024526

Tian, L., Yu, W., Schuster, P. F., Wen, R., Cai, Z., Wang, D., et al. (2020). Control of seasonal water vapor isotope variations at Lhasa, southern Tibetan Plateau. *Journal of Hydrology*, *580*, 124237. https://doi.org/10.1016/j.jhydrol.2019.124237

Tuinenburg, O. A., Hutjes, R. W. A., & Kabat, P. (2012). The fate of evaporated water from the Ganges basin. *Journal of Geophysical Research*, *117*, D01107. https://doi.org/10.1029/2011JD016221

Tuinenburg, O. A., Hutjes, R. W. A., Stacke, T., Wiltshire, A., & Lucas-Picher, P. (2014). Effects of irrigation in India on the atmospheric water budget. *Journal of Hydrometeorology*, *15*(3), 1028–1050. https://doi.org/10.1175/JHM-D-13-078.1

Wang, B., & LinHo (2002). Rainy season of the Asian-Pacific summer monsoon. *Journal of Climate*, *15*(4), 386–398. https://doi.org/10.1175/1520-0442(2002)015<0386:RSOTAP>2.0.CO;2

Xavier, P., Marzin, C., & Goswami, B. (2007). An objective definition of the Indian summer monsoon season and a new perspective on the ENSO-monsoon relationship. *Quarterly Journal of the Royal Meteorological Society*, *133*(624 PART A), 749–764.

Yao, T., Masson-Delmotte, V., Gao, J., Yu, W., Yang, X., Risi, C., et al. (2013). A review of climatic controls on δ18O in precipitation over the Tibetan Plateau: Observations and simulations. *Reviews of Geophysics*, *51*, 525–548. https://doi.org/10.1002/rog.20023

Yatagai, A., Kamiguchi, K., Arakawa, O., Hamada, A., Yasutomi, N., & Kitoh, A. (2012). APHRODITE: Constructing a long-term daily gridded precipitation dataset for Asia based on a dense network of rain gauges. *Bulletin of the American Meteorological Society*, *93*(9), 1401–1415. https://doi.org/10.1175/BAMS-D-11-00122.1